

New Measurements of the $\frac{\Gamma(D^+ \rightarrow \bar{K}^{*0} \mu^+ \nu)}{\Gamma(D^+ \rightarrow K^- \pi^+ \pi^+)}$ and $\frac{\Gamma(D_s^+ \rightarrow \phi \mu^+ \nu)}{\Gamma(D_s^+ \rightarrow \phi \pi^+)}$ Branching Ratios

The FOCUS Collaboration^{*}

J. M. Link^a M. Reyes^a P. M. Yager^a J. C. Anjos^b I. Bediaga^b
 C. Göbel^b J. Magnin^b A. Massafferri^b J. M. de Miranda^b
 I. M. Pepe^b A. C. dos Reis^b S. Carrillo^c E. Casimiro^c
 E. Cuautle^c A. Sánchez-Hernández^c C. Uribe^c F. Vázquez^c
 L. Agostino^d L. Cinquini^d J. P. Cumalat^d B. O'Reilly^d
 J. E. Ramirez^d I. Segoni^d J. N. Butler^e H. W. K. Cheung^e
 G. Chiodini^e I. Gaines^e P. H. Garbincius^e L. A. Garren^e
 E. Gottschalk^e P. H. Kasper^e A. E. Kreymer^e R. Kutschke^e
 L. Benussi^f S. Bianco^f F. L. Fabbri^f A. Zallo^f C. Cawlf^g
 D. Y. Kim^g K. S. Park^g A. Rahimi^g J. Wiss^g R. Gardner^h
 A. Kryemadhi^h K. H. Changⁱ Y. S. Chungⁱ J. S. Kangⁱ
 B. R. Koⁱ J. W. Kwakⁱ K. B. Leeⁱ K. Cho^j H. Park^j
 G. Alimonti^k S. Barberis^k A. Cerutti^k M. Boschini^k
 P. D'Angelo^k M. DiCorato^k P. Dini^k L. Edera^k S. Erba^k
 M. Giammarchi^k P. Inzani^k F. Leveraro^k S. Malvezzi^k
 D. Menasce^k M. Mezzadri^k L. Moroni^k D. Pedrini^k
 C. Pontoglio^k F. Prelz^k M. Rovere^k S. Sala^k
 T. F. Davenport III^l V. Arena^m G. Boca^m G. Bonomi^m
 G. Gianini^m G. Liguori^m M. M. Merlo^m D. Pantea^m
 S. P. Ratti^m C. Riccardi^m P. Vitulo^m H. Hernandezⁿ
 A. M. Lopezⁿ H. Mendezⁿ A. Parisⁿ J. Quinonesⁿ W. Xiongⁿ
 Y. Zhangⁿ J. R. Wilson^o T. Handler^p R. Mitchell^p D. Engh^q
 M. Hosack^q W. E. Johns^q M. Nehring^q P. D. Sheldon^q
 K. Stenson^q E. W. Vaandering^q M. Webster^q M. Sheaff^r

^aUniversity of California, Davis, CA 95616

^bCentro Brasileiro de Pesquisas Físicas, Rio de Janeiro, RJ, Brasil

^cCINVESTAV, 07000 México City, DF, Mexico

^dUniversity of Colorado, Boulder, CO 80309

^{*} See <http://www-focus.fnal.gov/authors.html> for additional author information.

^e*Fermi National Accelerator Laboratory, Batavia, IL 60510*

^f*Laboratori Nazionali di Frascati dell'INFN, Frascati, Italy I-00044*

^g*University of Illinois, Urbana-Champaign, IL 61801*

^h*Indiana University, Bloomington, IN 47405*

ⁱ*Korea University, Seoul, Korea 136-701*

^j*Kyungpook National University, Taegu, Korea 702-701*

^k*INFN and University of Milano, Milano, Italy*

^l*University of North Carolina, Asheville, NC 28804*

^m*Dipartimento di Fisica Nucleare e Teorica and INFN, Pavia, Italy*

ⁿ*University of Puerto Rico, Mayaguez, PR 00681*

^o*University of South Carolina, Columbia, SC 29208*

^p*University of Tennessee, Knoxville, TN 37996*

^q*Vanderbilt University, Nashville, TN 37235*

^r*University of Wisconsin, Madison, WI 53706*

Abstract

Using a large sample of charm semileptonic decays collected by the FOCUS photoproduction experiment at Fermilab, we present new measurements of two semileptonic branching ratios. We obtain values of $\frac{\Gamma(D^+ \rightarrow \bar{K}^{*0} \mu^+ \nu)}{\Gamma(D^+ \rightarrow K^- \pi^+ \pi^+)} = 0.602 \pm 0.010$ (stat) ± 0.021 (sys) and $\frac{\Gamma(D_s^+ \rightarrow \phi \mu^+ \nu)}{\Gamma(D_s^+ \rightarrow \phi \pi^+)} = 0.54 \pm 0.033$ (stat) ± 0.048 (sys). Our $D^+ \rightarrow \bar{K}^{*0} \mu^+ \nu$ result includes the effects of the s-wave interference discussed in Reference [1].

1 Introduction

This paper describes new measurements of charm semileptonic decay rates into the $D^+ \rightarrow \bar{K}^{*0} \mu^+ \nu$ and $D_s^+ \rightarrow \phi \mu^+ \nu$ final states relative to the hadronic decay rates $D^+ \rightarrow K^- \pi^+ \pi^+$ and $D_s^+ \rightarrow \phi \pi^+$ respectively. The $D^+ \rightarrow \bar{K}^{*0} \mu^+ \nu$ width sets the scale of the $A_1(0)$ form factor describing these decays [2] and therefore tests Lattice Gauge and quark model calculations. Such tests of the overall form factor scale are particularly relevant to the determination of CKM matrix element ratios such as $|V_{cd}/V_{cs}|^2$ which relates to (for example) $\Gamma(D^+ \rightarrow \rho \mu^+ \nu)/\Gamma(D^+ \rightarrow \bar{K}^* \mu^+ \nu)$. The $D_s^+ \rightarrow \phi \mu^+ \nu$ process has been frequently used to estimate the D_s^+ branching ratios via assumptions about $\Gamma(D_s^+ \rightarrow \phi \ell^+ \nu_\ell)$ since no high statistics double tag deduced branching fractions for the D_s^+ presently exist. Frequently the D_s^+ yields are established by counting $D_s^+ \rightarrow \phi \pi^+$ decays making a good measurement of $\Gamma(D_s^+ \rightarrow \phi \mu^+ \nu)/\Gamma(D_s^+ \rightarrow \phi \pi^+)$ important.

Recently the CLEO Collaboration obtained a new measurement of $\frac{\Gamma(D^+ \rightarrow \bar{K}^{*0} \ell^+ \nu_\ell)}{\Gamma(D^+ \rightarrow K^- \pi^+ \pi^+)}$ that is somewhat higher than previous measurements. They state in Reference [3], that their new value implies an increase in the ratio $\frac{\Gamma(D \rightarrow \bar{K}^* \ell^+ \nu)}{\Gamma(D \rightarrow K^- \ell^+ \nu)}$ bringing it more in line with early quark model estimates and in considerable discrepancy with the ISGW2 model [4]. This Letter discusses a more precise determination of the $\frac{\Gamma(D^+ \rightarrow \bar{K}^{*0} \mu^+ \nu)}{\Gamma(D^+ \rightarrow K^- \pi^+ \pi^+)}$ from FOCUS and provides a first measurement of this ratio that includes the effects of the interfering s-wave described in our recent paper [1]. The interference of this s-wave amplitude with the dominant $D^+ \rightarrow \bar{K}^{*0} \mu^+ \nu$ contribution to $D^+ \rightarrow K^- \pi^+ \mu^+ \nu$ significantly distorts the angular decay distributions thus affecting the reconstruction efficiency for this state. Throughout this paper, unless explicitly stated otherwise, the charge conjugate is also implied when a decay mode of a specific charge is stated.

2 Experimental and analysis details

The data for this paper were collected in the Wideband photoproduction experiment FOCUS during the Fermilab 1996–1997 fixed-target run. In FOCUS, a forward multi-particle spectrometer is used to measure the interactions of high energy photons on a segmented BeO target. The FOCUS detector is a large aperture, fixed-target spectrometer with excellent vertexing and particle identification. Most of the FOCUS experiment and analysis techniques have been described previously [5]. The FOCUS muon system and typical analysis cuts are described in References [6] and [1].

To isolate the $D^+ \rightarrow K^- \pi^+ \mu^+ \nu$ topology, we required that candidate muon, pion, and kaon tracks appeared in a secondary vertex with a confidence level exceeding 1%. The muon track, when extrapolated to the shielded arrays of

the inner muon system located downstream of both magnets, was required to match muon hits with a confidence level exceeding 5%. The kaon was required to have a Čerenkov light pattern more consistent with that for a kaon than that for a pion by 1 unit of log likelihood, while the pion track was required to have a light pattern favoring the pion hypothesis over that for the kaon by 1 unit [7].

To further reduce muon misidentification, a muon candidate was allowed to have no or one missing hit in the 6 planes comprising our inner muon system. In order to suppress muons from pions and kaons decaying in our spectrometer we required that muon candidates have an energy exceeding 10 GeV. Non-charm and random combinatoric backgrounds were reduced by requiring both a detachment between the vertex containing the $K^-\pi^+\mu^+$ and the primary production vertex of 10 standard deviations and a reconstructed energy between 40 and 180 GeV. Background from $D^+ \rightarrow K^-\pi^+\pi^+$, where a pion is misidentified as a muon, was reduced by requiring that the visible mass $m_{K\pi\mu} < 1.8 \text{ GeV}/c^2$. In order to suppress background from $D^{*+} \rightarrow D^0\pi^+ \rightarrow (K^-\mu^+\nu)\pi^+$ we required $M(K^-\mu^+\nu\pi^+) - M(K^-\mu^+\nu) > 0.18 \text{ GeV}/c^2$. The momentum of the undetected neutrino was estimated from the D^+ line-of-flight as discussed in Reference [1].

In addition to these cuts, that we will call “baseline” cuts, we imposed the following two cuts on the sample that we use to quote the branching ratio. To suppress possible backgrounds from higher multiplicity charm decay, we isolated the $K\pi\mu$ vertex from other tracks in the event (not including tracks in the primary vertex) by requiring that the maximum confidence level for another track to form a vertex with the candidate be less than 0.1%. To suppress background from the re-interaction of particles in the target region which can mimic a decay vertex, we required that the charm secondary vertex was located at least three measurement standard deviations outside of all solid material including our target and target microstrip system. We will call this the “out-of-material” cut.

Apart from the muon cuts and the cut on the $M(K^-\mu^+\nu\pi^+) - M(K^-\mu^+\nu)$ mass difference, these same cuts were applied to our $D^+ \rightarrow K^-\pi^+\pi^+$ sample. We required one of the two pions in the $D^+ \rightarrow K^-\pi^+\pi^+$ final state to be in the inner muon system to better match the angular region required for the muon in $D^+ \rightarrow K^-\pi^+\mu^+\nu$ events.

We turn next to a discussion of the cuts used in the $D_s^+ \rightarrow \phi \mu^+\nu$ analysis. Most of the cuts used for the $D^+ \rightarrow K^-\pi^+\mu^+\nu$ and $D^+ \rightarrow K^-\pi^+\pi^+$ selection were used to select our $\phi\mu^+\nu$ and $\phi\pi^+$ samples. Because the D_s^+ lifetime is shorter than the D^+ , we reduced our cut on the primary-secondary vertex detachment to greater than 5 standard deviations. To further reduce non-charm background we required that our primary vertex consisted of at least two charged tracks. To further reduce muon contamination to the $D_s^+ \rightarrow \phi \mu^+\nu$ state due to decays of pions and kaons in flight, we required that the confidence

level that a muon track had a consistent trajectory through the two magnets comprising the FOCUS magnetic spectrometer exceeded 5%.

3 Analysis of the $D^+ \rightarrow \bar{K}^{*0} \mu^+ \nu$ final state

Figure 1 shows the $K^- \pi^+$ mass distributions and fits of the signal we obtained using two selections of the cuts described above. A very strong \bar{K}^{*0} (896) signal is present for both samples. To assess the level of non-charm backgrounds, we plot the “right-sign” (where the kaon and muon have the opposite charge) and “wrong-sign” $K^- \pi^+$ mass distributions separately in Figure 1 (a) and (c) for the sample with the baseline cuts and the sample with baseline, out-of-material, and isolation cuts respectively. We attribute the dramatic decrease in the wrong sign component in Figure 1 (c) compared to Figure 1 (a) to a reduction in non-charm backgrounds through the use of the out-of-material cut.

The fits to the subtracted $K^- \pi^+$ mass distribution shown Figure 1 (b) and (d) are used to estimate the yield of $D^+ \rightarrow \bar{K}^{*0} \mu^+ \nu$ events. Two subtractions are applied. We first subtract the distributions of wrong-sign from right-sign events as a means of subtracting non-charm backgrounds that are nearly charge symmetric. We then subtract the anticipated right-sign excess predicted by our Monte Carlo simulation which simulates all known charm decay backgrounds. The Monte Carlo distribution used in this subtraction is scaled by the ratio of the fitted yield of $D^+ \rightarrow K^- \pi^+ \pi^+$ events observed in the data to that observed in the Monte Carlo. This second subtraction both simplifies the shape of the non- \bar{K}^{*0} component of the observed $K^- \pi^+$ mass spectrum and corrects for the presence of \bar{K}^{*0} 's from charm sources other than $D^+ \rightarrow \bar{K}^{*0} \mu^+ \nu$ such as hadronic charm decays where one of the secondaries is misidentified as a muon.

The fits overlaid on Figure 1 (b) and (d) are relativistic Breit-Wigner line shapes plus a 1st order polynomial of the form $\alpha(m_{K\pi} - m_o) + \beta$ where m_o is the pole mass of the \bar{K}^{*0} . The range of the fit is $0.7 < m_{K\pi} < 1.1 \text{ GeV}/c^2$. The fit parameters were the resonant Breit-Wigner mass, yield, and width and the α and β background parameters.

We found the subtracted data better fit a constant width Breit-Wigner with a mass and width consistent with the known[8] parameters of the \bar{K}^{*0} rather than the conventional p-wave form. We performed a variant of the subtracted $K^- \pi^+$ fit where the width was allowed to vary with mass according to $\Gamma(m_{K\pi}) = \Gamma_o(p/p_o)^N$ where p is the kaon momentum in the kaon-pion rest frame at a given $m_{K\pi}$, p_o is value of this momentum when the kaon-pion mass equals the resonant mass m_o and the power N was a fit parameter. We found that the data was very consistent with the power $N = 0$ and inconsistent (at the 20σ

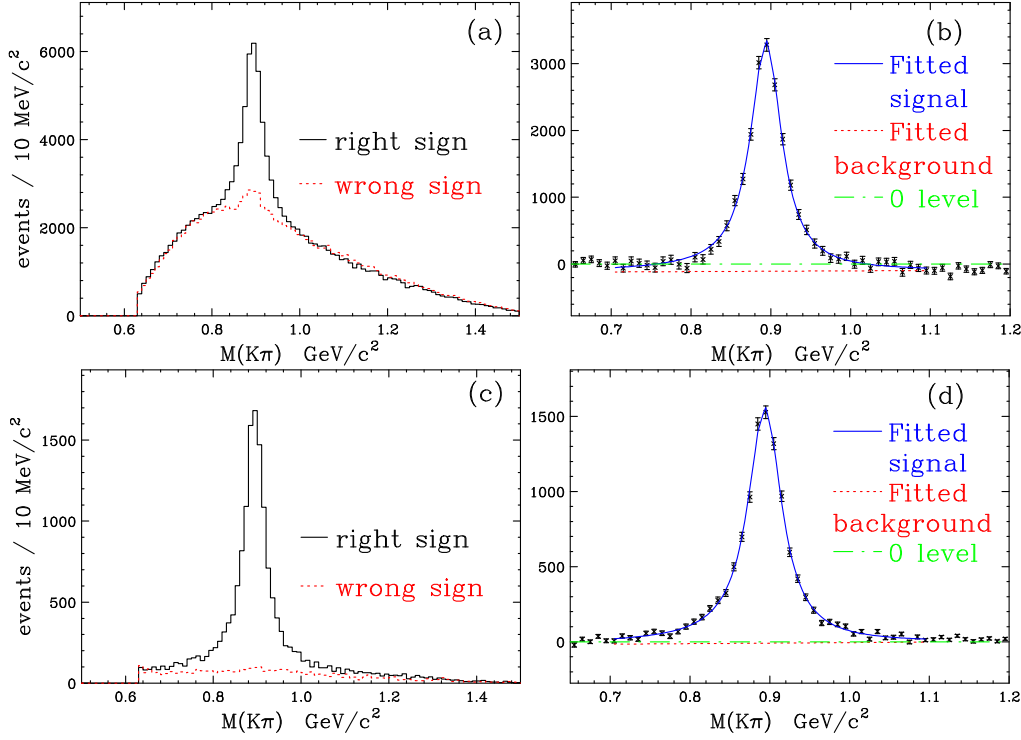


Fig. 1. We show two $D^+ \rightarrow K^* \mu \nu$ signals and fits (a) The $K^- \pi^+$ mass spectra subjected to the baseline cuts. The right-sign signal is plotted in a solid line and wrong-sign signal is plotted in a dotted line. (b) Fits to the subtracted baseline signal (described in the text). Both the wrong-sign, and charm backgrounds are subtracted prior to fitting. The fit, described in the text, consists of a Breit-Wigner plus a 1st order polynomial. The $D^+ \rightarrow \bar{K}^{*0} \mu^+ \nu$ yield obtained from this fit consists of 23 726 events. (c) The $K^- \pi^+$ mass spectra with an additional out-of-material cut and secondary isolation cut. The right-sign signal is plotted in a solid line and wrong-sign signal is plotted in a dotted line. (d) Fits to the baseline signal with additional out-of-material and secondary isolation cut. The $D^+ \rightarrow \bar{K}^{*0} \mu^+ \nu$ yield obtained from this fit consists of 11 698 events.

level) with $N = 3$ – the value expected for a p-wave Breit Wigner. We plan to present, in a subsequent publication, a detailed analysis of the $m_{K\pi}$ line shape in $D^+ \rightarrow \bar{K}^{*0} \mu^+ \nu$ decays including the effects of interference from the s-wave amplitude [1] and possible other sources, efficiency variation, and mass dependent form factor and barrier corrections.

Figure 1 (b) shows the presence of a significant negative offset (β) that is nearly absent in 1 (d) which we attribute to a broad structure excess of wrong-sign events in our non-charm background. The $D^+ \rightarrow K^- \pi^+ \pi^+$ yield was determined by fitting the $K^- \pi^+ \pi^+$ mass distributions to a Gaussian peak over a polynomial background. Figure 2 shows these fits for the baseline sample and the sample with the additional out-of-material and isolation cuts. The $\frac{\Gamma(D^+ \rightarrow \bar{K}^{*0} \mu^+ \nu)}{\Gamma(D^+ \rightarrow K^- \pi^+ \pi^+)}$ branching ratio is derived by dividing the fitted \bar{K}^{*0} yield in $D^+ \rightarrow \bar{K}^{*0} \mu^+ \nu$ events by the fitted $D^+ \rightarrow K^- \pi^+ \pi^+$ peak yield in data and then comparing to that obtained in our Monte Carlo with a known input

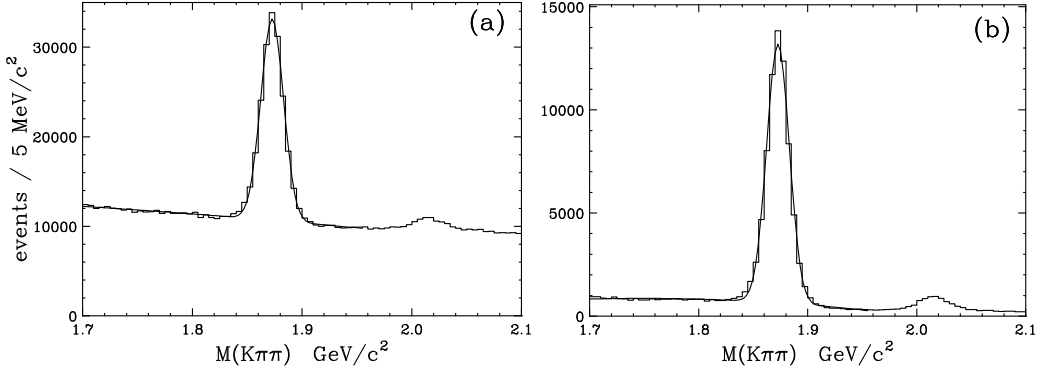


Fig. 2. We show two fitted $D^+ \rightarrow K^- \pi^+ \pi^+$ signals and fits (a) The $K^- \pi^+ \pi^+$ mass spectra subjected to the baseline cuts. The yield obtained from this fit is D^+ yield of 116 748 events. (b) The $K^- \pi^+ \pi^+$ mass spectra with an additional out-of-material cut and secondary isolation cut. The yield obtained from this fit is D^+ yield of 65 421 events. The peak near 2.01 GeV/c^2 is from the decay $D^{*+} \rightarrow D^0 \underline{\pi}^+ \rightarrow (K^- \pi^+) \underline{\pi}^+$ where the $\underline{\pi}$ pion is included in the primary vertex thus mimicking the $D^+ \rightarrow K^- \pi^+ \pi^+$ decay topology.

branching ratio. Because our $D^+ \rightarrow K^- \pi^+ \mu^+ \nu$ simulation model has an s-wave amplitude interfering with $D^+ \rightarrow \bar{K}^{*0} \mu^+ \nu$, we correct our ratio by a factor of 0.945, the fraction of Monte Carlo events due to the $D^+ \rightarrow \bar{K}^{*0} \mu^+ \nu$ process alone. We compute the numerator of this fraction, by integrating over the $K^- \pi^+ \mu^+ \nu$ phase space the model intensity discussed in Reference [1] with the s-wave amplitude set to zero. We then divide this numerator by the intensity integral where both the s-wave amplitude and \bar{K}^{*0} amplitudes are set to their proper values according to Reference [1]. This approach is frequently used in charm Dalitz plot analyzes to assess the fractional contributions of various quasi-two-body decay channels such as $D_s^+ \rightarrow \phi \pi^+$ even though these channels should be described by their quantum mechanical amplitudes rather than partial decay rates. After this correction, we obtain $\frac{\Gamma(D^+ \rightarrow \bar{K}^{*0} \mu^+ \nu)}{\Gamma(D^+ \rightarrow K^- \pi^+ \pi^+)} = 0.602 \pm 0.010$ where the quoted error is statistical only based on our samples with baseline, out-of-material and isolation cuts.

Three basic approaches were used to determine the systematic error on $\frac{\Gamma(D^+ \rightarrow \bar{K}^{*0} \mu^+ \nu)}{\Gamma(D^+ \rightarrow K^- \pi^+ \pi^+)}$. In the first approach, we measured the stability of the branching ratio with respect to variations in analysis cuts designed to suppress backgrounds. In these studies we varied the secondary isolation cut, the detachment cut, and a cut on the number of tracks in our primary vertex. The square root of the sample variance of the branching ratio from 8 such cut sets was 0.71 times our statistical error. In the second approach, we split our sample according to a variety of cuts applied to both the $D^+ \rightarrow K^- \pi^+ \mu^+ \nu$ numerator and $D^+ \rightarrow K^- \pi^+ \pi^+$ denominator and estimated a systematic based on the consistency of the branching ratio among the split samples. We split our sample based on the reconstructed D^+ momentum, particle versus antiparticle, and the sum of the energy of D^+ secondary tracks that would strike our calorimeter and thus contribute to our hadronic trigger. We chose these variables since

they significantly influence our acceptance. For example the D^+ momentum is tied to both our geometrical acceptance, and particle identification efficiencies. The calorimetric energy for a fixed D^+ momentum is significantly lower for the $D^+ \rightarrow K^- \pi^+ \mu^+ \nu$ than the $D^+ \rightarrow K^- \pi^+ \pi^+$ final state. The maximum systematic error for these splits was 1.57 times our statistical error. In the third approach we checked the stability of the branching fraction as we varied specific parameters in our Monte Carlo model and fitting procedure. These included varying the level of the background Monte Carlo prior to subtracting, the power of the momentum dependence of the width in the Breit-Wigner line shape as discussed previously, and the value of the three form factor ratios that describe the $D^+ \rightarrow \bar{K}^{*0} \mu^+ \nu$ decay distribution. We estimate a combined systematic from line shape, background level, and form factor systematic that is also 1.57 times our statistical error. Combining all three systematic error estimates in quadrature we have:

$$\frac{\Gamma(D^+ \rightarrow \bar{K}^{*0} \mu^+ \nu)}{\Gamma(D^+ \rightarrow K^- \pi^+ \pi^+)} = 0.602 \pm 0.010 \text{ (stat)} \pm 0.021 \text{ (sys)}$$

We believe that our systematic error estimate is conservative.

4 Analysis of the $D_s^+ \rightarrow \phi \mu^+ \nu$ final state

Figure 3 shows the $K^- K^+$ mass distributions that we obtained using two versions of the cuts described above. Figures 3 (a) and (c) compare the $K^+ K^-$ mass spectra for $D_s^+ \rightarrow \phi \mu^+ \nu$ candidates and in a charm background Monte Carlo normalized to the observed number of $D_s^+ \rightarrow \phi \pi^+$ events where the $D_s^+ \rightarrow \phi \mu^+ \nu$ contribution is excluded. The use of the out-of-material and isolation cuts both significantly reduces the ϕ background level and increases the agreement between the observed and that predicted background from charm sources according to our Monte Carlo. The difference of the fitted ϕ yields between the data and background Monte Carlo is the yield of ϕ that we will attribute to $D_s^+ \rightarrow \phi \mu^+ \nu$.

Figures 3 (b) and (d) compare the $K^+ K^-$ mass spectra for $D_s^+ \rightarrow \phi \pi^+$ candidates in a D_s^+ signal region and a sideband region based on the $K^+ K^- \pi^+$ invariant mass. The difference in fitted ϕ yields between the signal and sideband $K^+ K^-$ mass spectra will form our estimate of the $D_s^+ \rightarrow \phi \pi^+$ yield.

The $\frac{\Gamma(D_s^+ \rightarrow \phi \mu^+ \nu)}{\Gamma(D_s^+ \rightarrow \phi \pi^+)}$ branching ratio was derived by dividing the background subtracted, fitted ϕ yield in $D_s^+ \rightarrow \phi \mu^+ \nu$ events by the sideband subtracted, fitted ϕ yield in data and then comparing to the ratio obtained in our Monte Carlo with a known input branching ratio. We obtained $\frac{\Gamma(D_s^+ \rightarrow \phi \mu^+ \nu)}{\Gamma(D_s^+ \rightarrow \phi \pi^+)} = 0.54 \pm 0.033$ where the quoted error is statistical only based on our samples with baseline, out-of-material and isolation cuts.

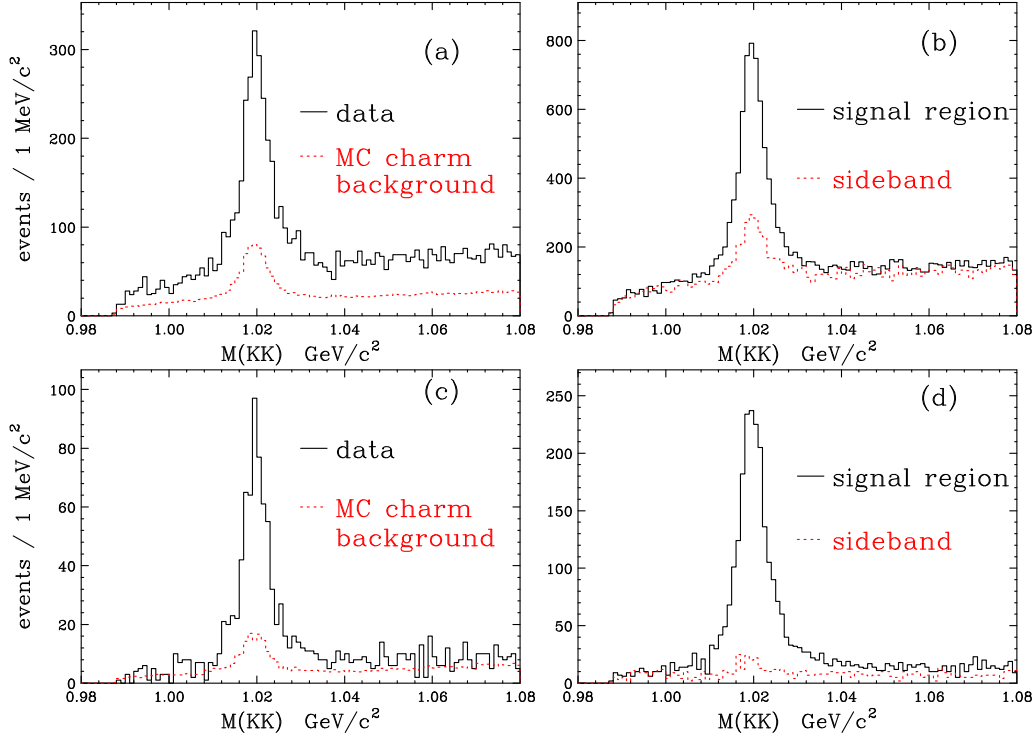


Fig. 3. We show signals for $D_s^+ \rightarrow \phi \mu^+ \nu$ and $D_s^+ \rightarrow \phi \pi^+$ (a) The K^-K^+ mass spectra in $D_s^+ \rightarrow \phi \mu^+ \nu$ events subjected to the baseline cuts. The data is plotted in a solid line and the background Monte Carlo is plotted in a dotted line. The difference in the fitted ϕ yield in the data and that in the background Monte Carlo is 2682 events. (b) The K^-K^+ mass spectra in $D_s^+ \rightarrow \phi \pi^+$ events subjected to the baseline cuts. The spectra for the D_s^+ signal region ($1.946 \text{ GeV}/c^2 < m_{KK\pi} < 1.996 \text{ GeV}/c^2$) is plotted in a solid line and the sideband region ($1.913 \text{ GeV}/c^2 < m_{KK\pi} < 1.938 \text{ GeV}/c^2$ and $2.004 \text{ GeV}/c^2 < m_{KK\pi} < 2.029 \text{ GeV}/c^2$) is plotted in a dotted line. The difference between the fitted ϕ yields in the signal and sideband region is 4695 events. (c) The K^-K^+ mass spectra in $D_s^+ \rightarrow \phi \mu^+ \nu$ events subjected to the baseline, out-of-material, and isolation cuts. The background subtracted ϕ yield is 793 events. (d) The K^-K^+ mass spectra in $D_s^+ \rightarrow \phi \pi^+$ events subjected to the baseline, out-of-material, and isolation cuts. The sideband subtracted ϕ yield is 2192 events.

The systematic error on the $\frac{\Gamma(D_s^+ \rightarrow \phi \mu^+ \nu)}{\Gamma(D_s^+ \rightarrow \phi \pi^+)}$ branching fraction was determined in a way similar to that used for the $D^+ \rightarrow \bar{K}^{*0} \mu^+ \nu$. The systematic error estimate obtained by varying analysis cuts was 1.06 times the statistical error. The systematic error estimate by splitting samples was 1.12 times the statistical error. The final estimate due to varying fit parameters such as the charm background level was 0.94 times the statistical error. Combining all three sources we have:

$$\frac{\Gamma(D_s^+ \rightarrow \phi \mu^+ \nu)}{\Gamma(D_s^+ \rightarrow \phi \pi^+)} = 0.54 \pm 0.033 \text{ (stat)} \pm 0.048 \text{ (sys)}$$

5 Summary

Table 1

Measurements of the $\frac{\Gamma(D^+ \rightarrow \bar{K}^{*0} \ell^+ \nu_\ell)}{\Gamma(D^+ \rightarrow K^- \pi^+ \pi^+)}$ branching fraction

Group	electron	muon
This work		$0.602 \pm 0.010 \pm 0.021$
CLEO [3]	$0.74 \pm 0.04 \pm 0.05$	$0.72 \pm 0.10 \pm 0.06$
CLEO [9]	$0.67 \pm 0.09 \pm 0.07$	
E687 [10]		$0.56 \pm 0.04 \pm 0.06$
OMEGA [11]	$0.62 \pm 0.15 \pm 0.09$	
ARGUS [12]	$0.55 \pm 0.08 \pm 0.10$	
E653 [13]		$0.46 \pm 0.07 \pm 0.08$
E691 [14]	$0.49 \pm 0.04 \pm 0.05$	

Table 1 summarizes measurements of the $\frac{\Gamma(D^+ \rightarrow \bar{K}^{*0} \ell^+ \nu_\ell)}{\Gamma(D^+ \rightarrow K^- \pi^+ \pi^+)}$ branching fraction for electrons and muons. Our measurement is the first one to include the effects on the acceptance due to changes in the decay angular distribution brought about by the s-wave interference [1]. After correcting the muon numbers by a factor of 1.05 to compare to electrons according to the prescription of Reference [8], we find that all values in the table are consistent with their weighted average (0.62 ± 0.02) with a confidence level of 19% if systematic errors are added in quadrature with statistical errors. Our number is about 1.57 standard deviations below the recent CLEO measurement and about 2.1 standard deviations above the number obtained by E691 [14].

Table 2

Measurements of the $\frac{\Gamma(D_s^+ \rightarrow \phi \ell^+ \nu_\ell)}{\Gamma(D_s^+ \rightarrow \phi \pi^+)}$ branching fraction

Group	electron	muon
This work		$0.54 \pm 0.033 \pm 0.048$
CLEO2 [15]	$0.54 \pm 0.05 \pm 0.04$	
E687 [16]		$0.58 \pm 0.17 \pm 0.07$
ARGUS [12]	$0.57 \pm 0.15 \pm 0.15$	
CLEO [17]	$0.49 \pm 0.10 \pm 0.12$	

Table 2 summarizes measurements of the $\frac{\Gamma(D_s^+ \rightarrow \phi \ell^+ \nu_\ell)}{\Gamma(D_s^+ \rightarrow \phi \pi^+)}$ branching fraction. All results are remarkably consistent with an average of 0.54 ± 0.04 .

6 Acknowledgments

We wish to acknowledge the assistance of the staffs of Fermi National Accelerator Laboratory, the INFN of Italy, and the physics departments of the collaborating institutions. This research was supported in part by the U. S. National Science Foundation, the U. S. Department of Energy, the Italian Istituto Nazionale di Fisica Nucleare and Ministero dell'Università e della Ricerca Scientifica e Tecnologica, the Brazilian Conselho Nacional de Desenvolvimento Científico e Tecnológico, CONACyT-México, the Korean Ministry of Education, and the Korean Science and Engineering Foundation.

References

- [1] FOCUS Collab. (J.M. Link et al.), Phys. Lett. B 535 (2002) 43.
- [2] J.G. Korner and G.A. Schuler, Z. Phys. C 46 (1990) 93.
- [3] CLEO Collab., *Measurement of the $D^+ \rightarrow \bar{K}^{*0} \ell^+ \nu_\ell$ Branching Fraction*, Mar 20, 2002, hep-ex/0203030.
- [4] D. Scora and N. Isgur, Phys. Rev. D 62 (1995) 2783.
- [5] See for example, J. M. Link et al., Phys. Lett. B 485 (2000) 62-70, and references therein.
- [6] E687 Collab., P. L. Frabetti et al., Nucl. Instrum. Meth. A 320 (1992) 519.
- [7] FOCUS Collab., J. M. Link et al., Nucl. Instrum. Meth. A 484 (2002) 270.
- [8] Particle Data Group, J. Bartels et al., Eur. Phys. J. C **15** (2000) 1.
- [9] CLEO Collab., A. Bean et al., Phys. Lett. B 317 (1993) 647.
- [10] E687 Collab., P. L. Frabetti et al., Phys. Lett. B 307 (1993) 262.
- [11] CERN WA82 Collab., M. Adamovich et al., Phys. Lett. B 268 (1991) 142.
- [12] Argus Collab., H. Albrecht et al., Phys. Lett. B 255 (1991) 634.
- [13] E653 Collab., K. Kodama et al., Phys. Lett. B 286 (1992) 187.
- [14] E691 Collab., J. C. Anjos et al., Phys. Rev. Lett. 62 (1989) 62.
- [15] CLEO Collab., F. Butler et al., Phys. Lett. B 324 (1994) 255.
- [16] E687 Collab., P. L. Frabetti et al., Phys. Lett. B 313 (1993) 253.
- [17] CLEO Collab., J. Alexander et al., Phys. Rev. Lett. 65 (1990) 1531.